Biomaterials 30 (2009) 1246–1253

Contents lists available at ScienceDirect

Biomaterials

journal homepage: www.elsevier.com/locate/biomaterials

Protamine sulfate/poly(L-aspartic acid) polyionic complexes self-assembled via electrostatic attractions for combined delivery of drug and gene

Han Cheng, Yong-Yong Li, Xuan Zeng, Yun-Xia Sun, Xian-Zheng Zhang*, Ren-Xi Zhuo

Key Laboratory of Biomedical Polymers of Ministry of Education, Department of Chemistry, Wuhan University, Wuhan 430072, PR China

ARTICLE INFO

Article history:
Received 15 August 2008
Accepted 7 November 2008
Available online 28 November 2008

Keywords:
Polyionic complex
Non-viral gene vector
Drug release
Combined delivery

ABSTRACT

In this study, a series of self-assembled polyionic complexes (PICs) were prepared via electrostatic attraction between protamine sulfate (PS) and poly(L-aspartic acid) (PASP) or doxorubicin (DOX)-conjugated PASP (DOX-PASP). The size of the PICs measured by Nano-ZS ZEN3600 was around 200–300 nm at different weight ratios of PS/PASP. Transmission electron microscopy (TEM) showed that PS/PASP PICs displayed a regular spherical shape and no aggregation was observed. The cytotoxicity study indicated that the PICs did not exhibit apparent cytotoxicity in comparison with that of 25 kDa polyethylenimine (PEI). Gel retardation assay indicated that the PICs were able to bind DNA completely when weight ratio of PS/PASP was higher than 2:1. Luciferase assay and green fluorescent protein (GFP) detection were used to confirm that the PICs could be used as efficient non-viral gene vectors and they exhibited comparable transfection efficiency with the one of 25 kDa PEI. Furthermore, confocal laser scanning microscopy as well as suppression activity of DOX-conjugated PICs (DOX-PICs) showed that they could quickly release the loaded DOX into HeLa cells, indicating that PICs can be also used as carriers for combined delivery of drug and gene.

1. Introduction

Non-viral gene vectors such as liposomes and cationic polymers allow the effective cure of diseased cells and tissues, as well as the controlled release of loaded therapeutic gene in the biological targets [1,2]. The use of drugs for the disease treatments has also led to new therapeutic strategies [3,4]. Combined delivery of drug and DNA was proposed to enhance gene expression or to achieve the synergistic effect of drug and gene therapies [5–8]. Nowadays, polyionic complexes (PICs) have demonstrated great potential in biomedical and biotechnological applications, including the controlled drug release [9–11], good biocompatibility [12] and DNA transfection [13–15].

PICs were composed of polycations and opposite polyanions. The polyionic particles have been prepared by many methods, such as microemulsion [16], inverse miniemulsion [17], self-assembly of biopolymers [18], and the intramolecular cross-linking of single chains of macromolecules [19]. Recently, a simple and green strategy was developed to form non-covalently connected PICs based on electrostatic attractions between natural macromolecules, for example, the ones composed of chitosan–ovalbumin, ovalbumin–lysozyme, lysozyme–dextran and ovalbumin–ovotransferrin [20–23]. An interesting property of PICs is that the net charges on the surface can be tuned by the weight ratio of macromolecules with opposite charges or pH. Thus, whether the PICs could be utilized as a non-viral gene vector and/or drug carrier seems very promising. Up to date, there have been very few reports in this regard.

Here, the doxorubicin (DOX)-conjugated PICs (DOX-PICs) based on poly(L-aspartic acid) (PASP) and protamine sulfate (PS) were prepared, and the potential to be used as gene vector and also drug carrier was investigated. The physiochemical properties of PICs were evaluated by the measurements of cytotoxicity, agarose gel electrophoresis, particle size, zeta potential and TEM. The in vitro gene transfection of PICs/DNA to different cell lines, as well as anti-tumor effect of DOX-PICs/DNA in terms of cell viability was examined. In addition, the cell internalization of DOX-PICs/DNA was investigated via confocal laser scanning microscopy.

2. Materials and methods

2.1. Materials

Protamine sulfate (PS) was purchased from Wuhan Life Technologies Co. (China). L-Aspartic acid and phosphoric acid were of analytical grade and used as supplied by Shanghai Chemical Co. (China). N,N′-Dimethylformamide (DMF) was obtained from Shanghai Chemical Reagent Co. and used after distillation under reduced pressure. N-(3-Dimethylaminopropyl)-N′-ethylcarbdiimide (EDC) was purchased from Sigma. Doxorubicin hydrochloride (DOX·HCl) was purchased from Zhejiang Hisun Pharmaceutical Co. (China). Plasmid pGL-3 control with SV40 promoter and enhancer sequences encoding luciferase was obtained from Promega, Madison, WI (USA). Plasmid pEGFP-C1 encoding a red-shifted variant of wild-type green fluorescent

* Corresponding author. Tel./fax: +86 27 6875 4059.
E-mail address: xz-zhang@whu.edu.cn (X.-Z. Zhang).

0142-9612/$ – see front matter © 2008 Elsevier Ltd. All rights reserved.
doi:10.1016/j.biomaterials.2008.11.002

protein (GFP) was purchased from Clontech, Mountain View, CA (USA). All other chemicals were of analytical grade and used as received.

2.2. Plasmid DNA preparation and purification

pGL-3 and pEGFP-C1 plasmids were used in the following study. The former one was transformed in *E. coli* JM109 and the latter one was transformed in *E. coli* DH5α. Both plasmids were amplified in Luria-Bertani (LB) medium at 37 °C overnight at 250 rpm. Then the plasmids were purified as described by means of EndoFree plasmid purification. The purified plasmids were diluted by TE buffer solution and stored at −20 °C. The integrity of plasmids was confirmed by agarose gel electrophoresis. The purity and concentration of plasmids were determined by ultraviolet (UV) absorbance at 260 and 280 nm, respectively.

2.3. Synthesis of PASP

PASP was synthesized according to the literature [24]. L-aspartic acid (29.5 g) was mixed with phosphoric acid (15.0 g) in a round-bottomed flask. The flask was placed in a rotary evaporator and heated under reduced pressure in an oil bath at 180 °C for 2.5 h. The mixture was then dissolved in 200 mL of DMF. Then solution was added to water slowly and white precipitate formed in this course. The precipitate was collected and washed with water till neutrality, then dried in vacuum at 110 °C for 24 h to obtain 18.1 g of poly(L-succinimide). The prepared poly(L-succinimide) was dissolved in 200 mL of DMF, and then added dropwise to a solution of 1 M NaOH to hydrolyze the succinimide units. The system was cooled in an ice bath. The mixture was stirred for 3 h, followed by dialyzing against hydrochloric acid solution and then against pure water. At last, the solution was freeze dried to obtain the final polymer.

2.4. DOX conjugation to PASP

200 mg PASP and 20 mg DOX were dissolved in 5 mL buffer solution (pH 6), then 13.2 mg EDC in 2 mL water was added. The reaction mixture was stirred overnight at room temperature. Then the mixture was dialyzed against pure water and the product was harvested by freeze-drying.

2.5. ^{1}H NMR measurement

^{1}H NMR spectra were recorded on a Varian Unity 300 MHz spectrometer and TMS was used as internal standard.

2.6. PICs formation

PASP solution (10 mg PASP or DOX-PASP in 10 mL PBS) was added into certain amount of PS solution (1 mg/mL) under agitation until the predetermined weight ratio of PS/PASP was reached, and the mixture solution was stirred slowly at room temperature for 2 h. This procedure of PICs preparation was applied throughout the present research and other conditions used are indicated specially.

2.7. PICs/DNA or DOX-PICs/DNA complex formation

A plasmid DNA stock solution (120 ng/μL) was prepared in Tris–HCl buffer solution (pH 7.4). PS solution and DNA stock solution were mixed to form complexes with different weight ratios. PASP solution (10 mg PASP or DOX-PASP in 10 mL PBS) was then added into PS/DNA solution until the predetermined weight ratio of PICs was reached. The formation of PICs/DNA or DOX-PICs/DNA complexes was completed in 30 min after mixing PS/DNA for 15 s and stay for 5 min. The total volume of each complex was adjusted to 100 μL with 150 mM PBS solution, respectively.

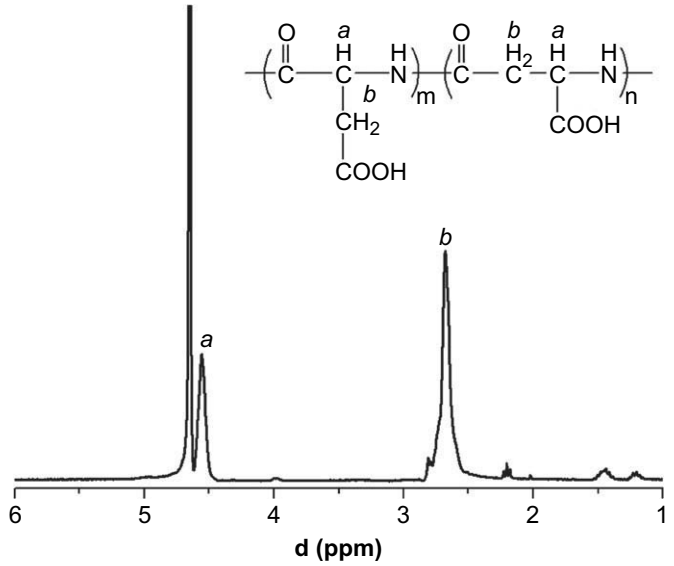

Fig. 1. The ^{1}H NMR spectra of poly(L-aspartic acid) (PASP).

2.8. Agarose gel retardation assay

PICs/DNA complexes at predetermined weight ratios were loaded on the 0.7% (w/v) agarose gel containing GelRed™ and with Tris–acetate (TAE) running buffer at 80 V for 80 min. DNA was visualized with an UV lamp using a Vilber Lourmat imaging system (France).

2.9. Particle size, stability and zeta potential measurement

The particle size of PICs was measured by Nano-ZS ZEN3600 (MALVERN Instr.). The stability test was performed by measuring the particle size of the PICs in each day during a 5-day storage. The zeta potential of PICs was measured using Nano-ZS ZEN3600 based on the principle of phase analysis light scattering. The PICs solution (250 mg/L) was passed through a 0.45 μm pore size filter before measurements and diluted if necessary according to the instrument's requirements.

2.10. TEM measurement

The morphologies of the PICs and PICs/DNA complexes were observed on transmission electron microscope (TEM JEM-100CXa) with an acceleration voltage of 100 kV. Before the TEM measurement, a drop of complex suspension was placed onto the copper grid, which had been precoated with a thin film of Formvar and then coated with carbon. After a few minutes, the excess solution was blotted away with filter paper. Then, a drop of 0.5% (w/v) phosphotungstic acid was placed on the above grids and kept for minutes, and the residual solution was removed by filter paper. The grid was dried at room temperature at atmospheric pressure for several hours before the observation.

2.11. Cell culture

Human embryonic kidney 293T cells (HEK293T), human cervix carcinoma cells (HeLa) and human hepatocellular carcinoma cells (HepG2) were incubated in Dulbecco's Modified Eagle's Medium (DMEM) containing 10% Fetal Bovine Serum (FBS) and 1% antibiotics (penicillin–streptomycin, 10,000 U/mL) at 37 °C in a humidified atmosphere containing 5% CO_2.

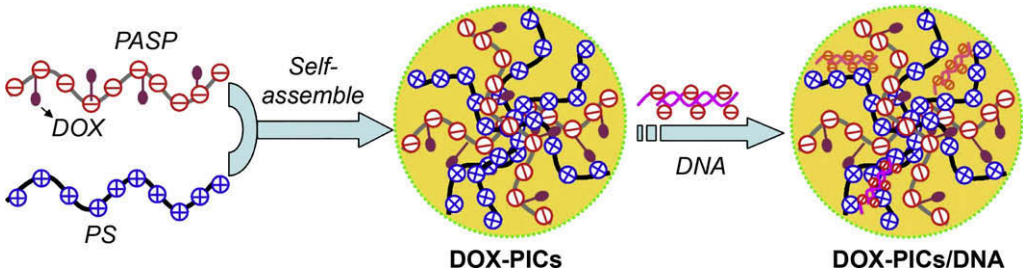

Scheme 1. Schematic illustration of the self-assembled protamine sulfate/doxorubicin-conjugated poly(L-aspartic acid) (PS/DOX-PASP) polyionic complexes (DOX-PICs) as drug and gene carriers.

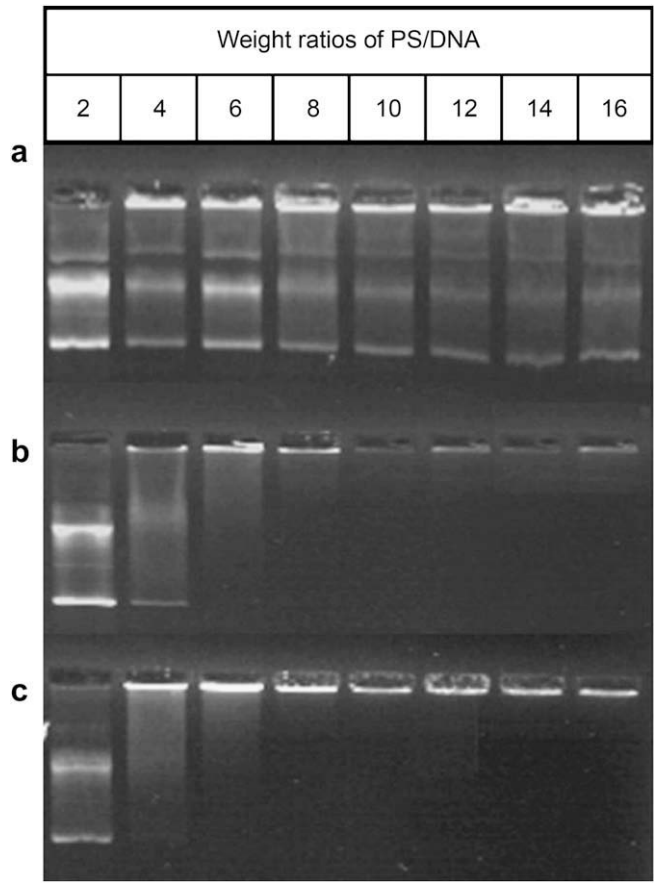

Fig. 2. Agarose gel electrophoresis retardation of plasmid DNA in PICs/DNA complexes with different weight ratios of (a) PS/PASP 1:1, (b) PS/PASP 2:1 and (c) PS/PASP 3:1 at varied PS/DNA weight ratios ranging from 2 to 16.

2.12. Cell viability assay

For cell viability assay, HEK293T cells (2500 cells/well), HeLa cells (2500 cells/well) and HepG2 cells (2500 cells/well) were seeded into 96-well micro titer plates. PICs or DOX-PICs were formed at different weight ratios and the cells were then incubated in culture medium containing PICs or DOX-PICs at various concentrations for 48 h. After that the medium was replaced with 200 μL of fresh medium and 20 μL of sterile filtered MTT (3-(4,5-dimethyl-thiazol-2-yl)-2,5-diphenyl tetrazolium bromide) (5 mg/mL) stock solution in PBS was added to each well reaching a final concentration of 0.45 mg/mL. After 4 h, unreacted dye was removed by aspiration. The formazan crystals were dissolved in 200 mL DMSO per well and measured spectrophotometrically in an ELISA plate reader (Model 550, Bio-Rad) at 570 nm. The cell viability in the presence of complexes was calculated as: Cell viability = $(OD_{treated}/OD_{control}) \times 100\%$, where $OD_{control}$ was obtained in the absence of PICs (or DOX-PICs) and $OD_{treated}$ was obtained in the presence of PICs (or DOX-PICs).

Table 1
Zeta potential of polyionic complexes (PICs) with varied PS/PASP weight ratios.

Weight ratio (PS/PASP)	1:1	2:1	3:1	4:1	5:1
Zeta potential (mV)	−28.5	−15.1	26.1	26.4	26.7

2.13. Gene transfection

For in vitro transfection study, the HEK293T cells, HeLa cells and HepG2 cells were split one day prior to transfection and plated in 24-well plates at a density of 5×10^4 cells/well. Before transfection, the cell culture medium was replaced with serum-free DMEM. The cells were transfected with gene loaded complexes containing 1 μg of plasmid DNA at 37 °C for 4 h, respectively. Then the complexes were removed and the cells were incubated in fresh DMEM with 10% FBS at 37 °C for another 48 h.

2.14. Luciferase assay

The cells were washed by PBS and lysed with the reporter lysis buffer (Promega, USA). The luciferase activity in cell extracts was measured using a luciferase assay kit (Promega, USA). Each measurement was carried out for 10 s in a single-well luminometer (Berthold Lumat LB 9507, Germany). The relative light units (RLU) were normalized by the total protein concentration of the cell extracts, and the total protein was measured with a BCA protein assay kit (PERBIO, USA). Luciferase activity was expressed as RLU/mg protein.

2.15. GFP detection

The cells expressing green fluorescent proteins were observed by inverted microscope (IX 70, OLYMPUS, JAPAN).

2.16. Confocal microscopy

Cells were seeded into specific confocal investigation plate containing 1 mL DMEM (1×10^5 cells/plate). Then, the cell samples were incubated with DOX-PICs containing 1 μg of plasmid DNA at 37 °C for 4 h. The fluorescent images of cells were analyzed using laser scanning confocal microscopy at wavelength of 405 nm and 488 nm, respectively.

3. Results and discussion

3.1. Synthesis of PASP and DOX-PASP

The synthesis of PASP involved two steps. Poly(L-succinimide) was initially synthesized and the removal of water is the key factor in this step. Then poly(L-aspartic acid) was prepared by hydrolysis of poly(L-succinimide) in alkaline solution. Fig. 1 shows the ^{1}H NMR spectrum of prepared PASP. In the spectrum of PASP, the typical

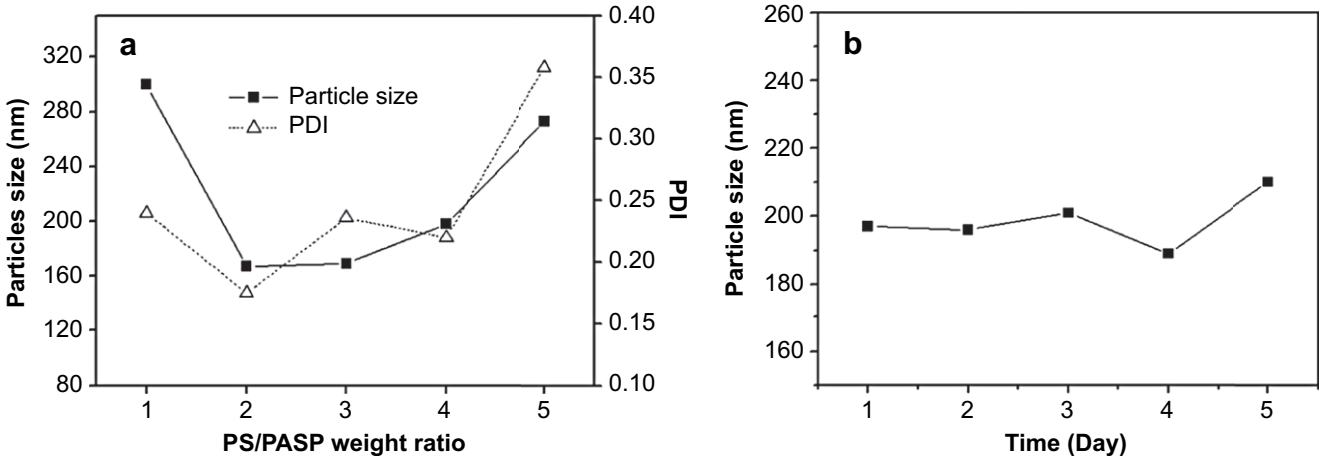

Fig. 3. (a) Particle size and polydispersity of PICs at different weight ratios of PS/PASP ranging from 1:1 to 5:1 and (b) particle size of PICs at weight ratio of PS/PASP 4:1 during the 5-day storage.

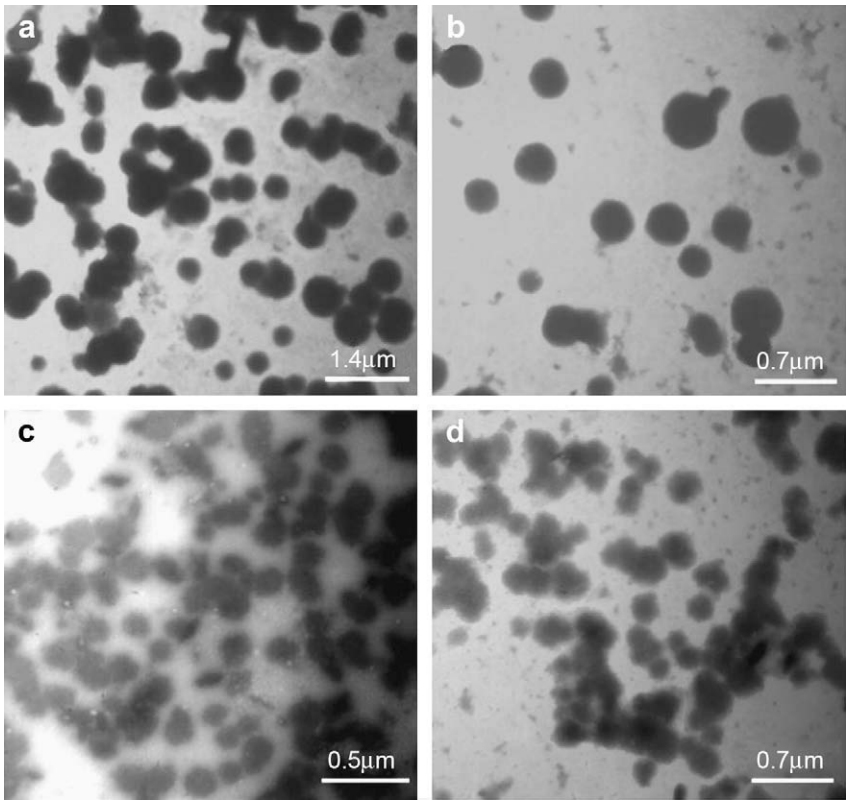

Fig. 4. TEM images of the PICs and PICs/DNA complexes. Images (a) and (b) showed the morphologies of PICs with different weight ratios of PS/PASP 3:1 (a), 4:1 (b), while images (c) and (d) showed the morphologies of PICs/DNA complexes with different weight ratios of PS/PASP/DNA 120:40:1 (c) and 120:30:1 (d).

signals at 4.4–4.6 ppm and 2.4–2.8 ppm were ascribed to hydrogen connected with nitrogen and carbonyl group, respectively. DOX-conjugated PASP was synthesized by a condensation reaction between PASP and DOX in PBS solution, and then purified by dialysis. The content of DOX (2.94 wt%) conjugated in DOX-PASP was obtained based on the standard curve by using the UV absorbance at 480 nm as reference (see Supplementary Information, Fig. S1). The number average molecular weight (Mn) of PASP calculated from GPC traces was 7700 with a PDI of 1.29 (see Supplementary Information, Fig. S2). The Mn of PASP was comparable with that of PS (6000–9000).

3.2. Formation of PICs

PS is mainly composed of poly(L-arginine acid) (PARG), which is biodegradable and has been widely used for biomedical and biotechnological applications. PS is a polycation, while PASP is a polyanion, electrostatic attraction happens between them. In this study, the self-assembly of PS and PASP was conducted in PBS buffer solution (pH 7.4). Under this condition, the above two macromolecules having opposite charges were found to self-assemble effectively into PICs. The self-assembly behavior of PS/DOX-PASP PICs was schematically illustrated in Scheme 1.

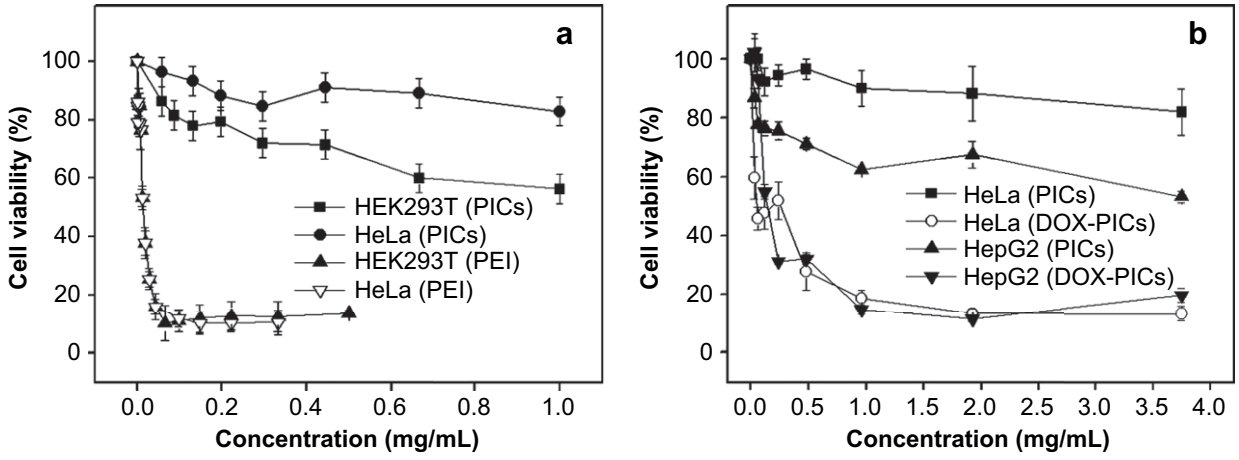

Fig. 5. (a) Viability of HEK293T cells and HeLa cells against PICs (PS/PASP 3:1) and 25 kDa PEI, and (b) the suppression to HeLa cells and HepG2 cells after being treated with PICs (PS/PASP 3:1) and DOX-PICs (PS/DOX-PASP 3:1). For cell suppression assay, the DOX concentrations of 0.22, 0.44, 0.88, 1.76, 3.53, 7.06, 14.11 and 27.6 μg/mL were corresponding to the DOX-PICs concentrations of 0.03, 0.06, 0.12, 0.24, 0.48, 0.96, 1.92 and 3.75 mg/mL, respectively.

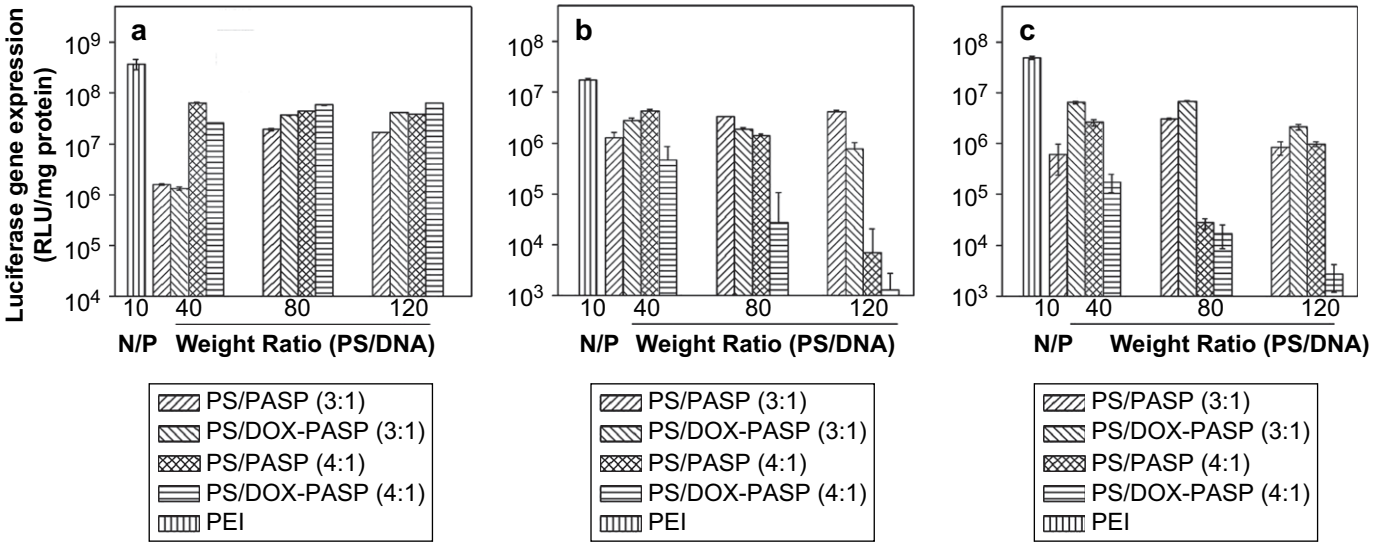

Fig. 6. Luciferase expression in HEK293T cells (a), HeLa cells (b) and HepG2 cells (c). Each kind of cells was transfected with PICs/DNA complexes at different PS/DNA weight ratios with PASP or DOX-PASP. For luciferase expression, at PS/DNA weight ratios of 40/1, 80/1 and 120/1, PICs concentrations were 53.3, 106.7 and 160 μg/mL, respectively, while the DOX concentrations were 0.39, 0.78 and 1.17 μg/mL, respectively at PS/DOX-PASP weight ratio of 3:1. In addition, PICs concentrations were 50, 100 and 150 μg/mL, respectively, while DOX concentrations were 0.29, 0.59 and 0.88 μg/mL, respectively at PS/DOX-PASP weight ratio of 4:1 with the corresponding PS/DNA weight ratios as noted above. 25 kDa PEI/DNA complexes at the optimal ratio (N/P = 10) were taken as control. Data were shown as mean ± SD ($n = 3$).

3.3. DNA-binding ability of PICs

The DNA-binding capability is a prerequisite for the gene vectors [25]. The condensed form of PICs/DNA complexes can protect the DNA against digestion by enzymes. In order to study the DNA-binding ability of PICs, we chose predetermined weight ratios of PS/PASP from 1:1 to 3:1 and examined the agarose gel electrophoresis of PICs/DNA complexes at varied weight ratio of PS/DNA. As shown in Fig. 2, the PICs efficiently associated DNA even at low weight ratios of PS/DNA with PS/PASP at 2:1 and 3:1. The complete retardation of DNA was achieved at PS/DNA weight ratio of 8 and 6 for PICs at PS/PASP 2:1 and 3:1, respectively, but it was difficult to bind DNA at any weight ratio of PS/DNA for PICs at PS/PASP 1:1. In addition, a stronger DNA-binding ability of PICs was observed at PS/PASP 3:1 than that of PS/PASP 2:1 due to different amount of positive charged PS. These results proved that the PICs can be used to bind DNA as gene vectors with two qualifications: a) the weight ratio of PS/PASP should be above 2, and b) the weight ratio of PS/DNA should be above 8.

3.4. Particle size measurement

The particle size of the PICs at different weight ratios of PS/PASP was shown in Fig. 3a. All the sizes of complexes were measured at weight ratios ranging from 1:1 to 5:1. At the lowest weight ratio, the particle size was around 300 nm. When the weight ratio increased from 1:1 to 2:1, the particle size decreased from 300 nm to 167 nm. Then, when the weight ratio further increased from 2:1

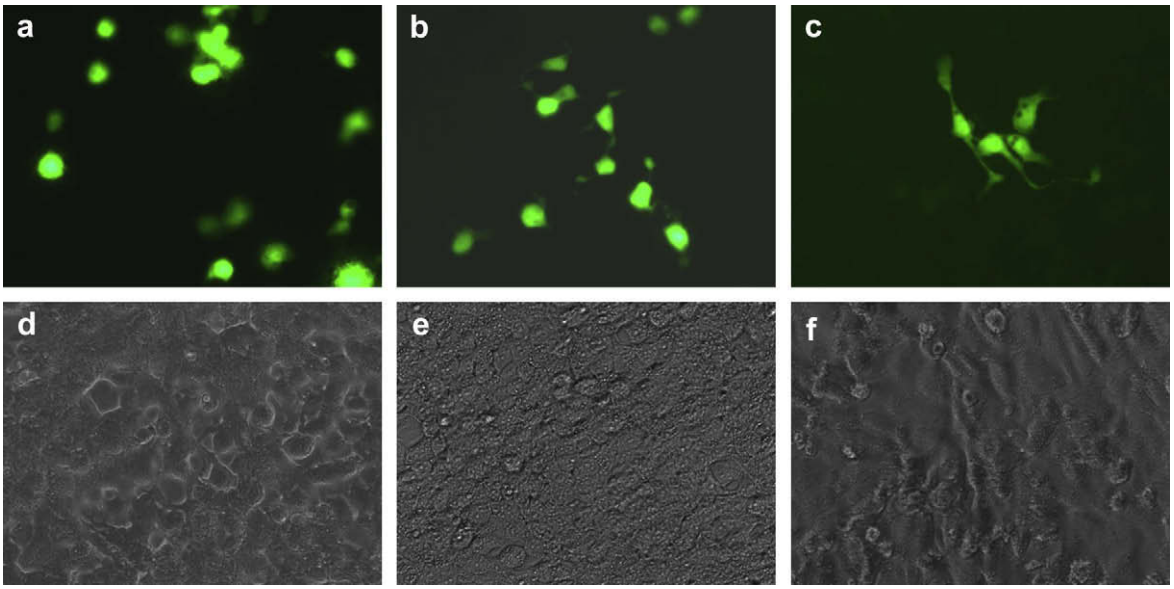

Fig. 7. GFP detection of the transfected HEK293T cells, HeLa cells and HepG2 cells. The images (a, b and c) were the fluorescent images, and the images (d, e and f) were the bright-field images. The images (a, d) were observed in HEK293T cells with PS/PASP/DNA weight ratio of 40:10:1, images (b, e) were observed in HeLa cells with PS/PASP/DNA weight ratio of 80:26.7:1 and images (c, f) were observed in HepG2 cells with PS/PASP/DNA weight ratio of 80:26.7:1. The images were obtained at a magnification of 100×.

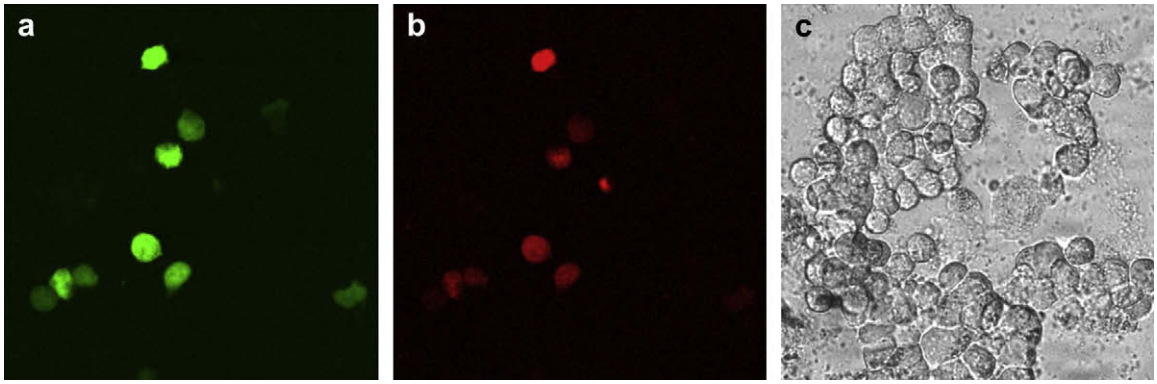

Fig. 8. The transfected HeLa cells by DOX-PICs/DNA complexes observed by confocus microscope. (a) Fluorescence green channel of EGFP, (b) fluorescence red channel of DOX, (c) under bright-field. The images were obtained at a magnification of 100×.

to 5:1, the particle size increased from 167 nm to 273 nm. In addition, as shown in Fig. 3a, PICs with PS/PASP 2:1 had a smallest PDI than that with other weight ratios. Obviously, the particle size of the complexes depends on weight ratios. It seems that there exists an equilibrium between PS and PASP. Too high or too low weight ratio of PS/PASP is not favorable to form a compact complex. Fig. 3a showed that PICs with PS/PASP weight ratio of 2:1 had a most compact structure. Since the PICs formation was controlled by the electrostatic attraction between PS and PASP, it was speculated that the PICs would have a loose structure due to that too excess charges exist when the weight ratio of PS/PASP deviated from 2:1.

The stability of PICs was also investigated. Taking PICs (PS/PASP 4:1) for example, as shown in Fig. 3b, during the first two days, particle size was almost unchanged, and even at the 5th day, PICs did not aggregate and their size remained lower than 210 nm. This means, the stable PICs can be prepared by electrostatic attraction with appropriate weight ratios of PS/PASP. Furthermore, the good stability of PICs supplied an opportunity for storage [26,27].

3.5. Zeta potential measurement

Zeta potential of the PICs, characterized by a zeta potential analyser with dynamic light-scattering capability, increased from −28.5 mV to 26.7 mV with the increasing weight ratio of PS/PASP from 1:1 to 5:1 as shown in Table 1. At a higher weight ratio of PS/PASP, the PICs possessed a higher zeta potential due to the increasing content of PS. The positive zeta potential of PICs made complexes easier to be uptaken by cells, attributed to the electrostatic interactions between negative charged cellular membranes and positive charged complexes [28,29].

3.6. TEM measurement

The morphology of PICs and PICs/DNA complexes was observed by TEM. It is evident from Fig. 4 that all the particles have a regular spherical shape. There is no aggregation and the morphology of the PICs/DNA complexes is as alike as the PICs. As exhibited in Fig. 4c and d, the particle size of the PICs/DNA complexes is approximate 250 nm, while the one of PICs is around 300 nm as shown in Fig. 4a and b.

3.7. Cytotoxicity of PICs

For gene therapy, gene vectors should not induce cytotoxic effects [30] and the low cytotoxicity of PICs is very important. Here, the cytotoxicity of PICs (PS/PASP 3:1) was evaluated in HEK293T cells and HeLa cells by MTT assay using 25 kDa PEI as the control. As shown in Fig. 5a, the viability of HEK293T cells and HeLa cells against PICs was above 80% even the concentration was 1.0 mg/mL, showing the much lower cytotoxicity of PICs when compared with that of 25 kDa PEI.

Then PICs (PS/PASP 3:1) and DOX-PICs (PS/DOX-PASP 3:1) were used as a contrastive pair to the tumor cells (HeLa cells and HepG2 cells) to demonstrate the suppression activity of DOX-PICs. As shown in Fig. 5b, the viability of HeLa cells with PICs was above 80% when the concentration was 1 mg/mL, while the cell viability decreased dramatically from 80% to 20% in the presence of DOX-PICs. Similar results were obtained in HepG2 cells when PICs was replaced by DOX-PICs, the cell viability decreased from 60% to 20% when the concentration was 1 mg/mL, which suggests that the conjugated DOX in DOX-PICs did achieve the similar anti-tumor effect as the free DOX did.

3.8. In vitro transfection

Transfection efficiency is correlated with cytotoxicity as well as particle size of the polymer/DNA complexes. The particle size is an important parameter for transfection efficiency. Generally, the smaller particle size would facilitate the cellular uptake and enhance transfection efficiency. Based on above results, PICs with appropriate weight ratios (PS/PASP 3:1 and 4:1) were chosen as gene vectors. The plasmid pGL-3 was used as the luciferase reporter gene and the luciferase expression efficiency induced by the PICs/DNA was investigated in HEK293T, HeLa and HepG2 cell lines. In order to examine the influence of different PS/PASP weight ratios on the transfection efficiency, the efficiency of PICs/DNA complexes was evaluated at weight ratios of PS/DNA from 40 to 120 in comparison with the efficiency of 25 kDa PEI at the optimal ratio (N/P ratio = 10). As shown in Fig. 6, the luciferase activities of PICs/DNA complexes depend on cell type and PICs composition. For instance, in HEK293T cell line, the gene expression level increased with increasing PS/DNA ratio for PICs with PS/PASP 3:1. Besides, between two PICs with different weight ratios of PS/PASP, PICs/DNA with PS/PASP 4:1 had the higher gene expression level at a PS/DNA ratio of 40, which was 48 times higher than that of PICs/DNA with PS/PASP 3:1 at the same PS/DNA ratio. However, with increasing PS/DNA ratios, the differences became much smaller (Fig. 6a).

In HeLa cell line, the results became different from those above. Although PICs/DNA with PS/PASP 4:1 yielded the highest gene expression level at the PS/DNA weight ratio of 40, the gene expression level of PICs/DNA with PS/PASP 3:1 was improved with increasing PS/DNA ratio, while the gene expression level of PICs

with PS/PASP 4:1 was decreased with increasing PS/DNA ratio (Fig. 6b). However, in HepG2 cell line, PICs/DNA with PS/PASP 3:1 had the highest gene expression level and PICs/DNA with PS/PASP 4:1 had the lowest one at the PS/DNA weight ratio of 80, which is different to the trend in HeLa cell line (Fig. 6c).

To further investigate whether the conjugated DOX affects the transfection efficiency, DOX-PICs were studied via the same process above. Similar phenomena were observed in HEK293T cells when PASP was replaced by DOX-PASP (Fig. 6a), but in HeLa and HepG2 cells the gene expression level of DOX-PICs/DNA decreased with increasing PS/DNA ratio (Fig. 6b and c). The results were ascribed to the tumor cell suppression of DOX in DOX-PICs. At PS/DNA weight ratios of 80 and 120, the concentration of DOX in DOX-PICs/DNA increased, thus the viability of tumor cells decreased with the increasing content of DOX. Since the cell viability is correlative with the transfection efficiency, the conjugated DOX would restrain the proliferation of the tumor cells during gene transfection, and further restrain the transfection efficiency. The findings demonstrated the ability of DOX-PICs to bind DNA, and thereafter delivery the drug and DNA to cells simultaneously.

In order to visualize the infected cells expressing GFP, the plasmid pEGFP-C1 was used as the green fluorescent protein reporter gene. pEGFP-C1 encodes a red-shifted variant of wild-type GFP with optimized brighter fluorescence and higher expression in mammalian cells. The green fluorescent cells were observed by inverted microscope at each optimal weight ratio of the PICs/DNA complexes. Clearly, GFP had been successfully expressed in these three types of cells (Fig. 7a–c).

To directly visualize whether the complexes could enter the tumor cells during the transfection process, HeLa cells were chosen for combined delivery assay and the cellular internalization of DOX-PICs/DNA complexes was also investigated. After 24 h of incubation with the DOX-PICs/DNA complexes, the HeLa cells were observed by a laser scanning confocal microscope using wavelength stimulated at 405 nm or 488 nm. As shown in Fig. 8, strong green fluorescent expressions can be observed, which means plasmid DNAs have been delivered into HeLa cells and the transfection occurred (Fig. 8a). The study also revealed the presence of red fluorescent DOX in the same cells, that is, the PICs released the conjugated DOX to HeLa cells synchronously (Fig. 8b). The qualitative results from fluorescent microscopy studies are in good agreement with the quantitative results obtained from above luciferase assay and cytotoxic assay, confirming the combined delivery of drug and gene in cells.

4. Conclusion

In this study, a series of PICs were prepared by the electrostatic attraction between PS and PASP. Compared with 25 kDa PEI, PICs exhibited much lower cytotoxicity. In vitro gene transfection investigation revealed that the transfection efficiency of PICs/DNA complexes was comparable to that of 25 kDa PEI/DNA complex (N/P ratio 10). Importantly, the gene transfection efficiency of PICs/DNA complexes could be tuned by altering the weight ratio of PS/PASP. The suppression of the proliferation activity of HeLa cells could be achieved by replacing PASP with DOX-PASP, suggesting a great potential of PICs as effective carriers for combined delivery of drug and gene.

Acknowledgements

This work was supported by National Natural Science Foundation of China (20774069) and Ministry of Education of China (Cultivation Fund of Key Scientific and Technical Innovation Project 707043).

Appendix A. Supplementary data

Supplementary data associated with this article can be found, in the online version, at doi:10.1016/j.biomaterials.2008.11.002.

Appendix

Figures with essential colour discrimination. Figures 7 and 8 in this article are difficult to interpet in black and white. The full colour images can be found in the on-line version, at doi: 10.1016/j.biomaterials.2008.11.002.

References

[1] Kichler A. Gene transfer with modified polyethylenimines. J Gene Med 2004;6:S3–10.
[2] Kircheis R, Wightman L, Wagner E. Design and gene delivery activity of modified polyethylenimines. Adv Drug Deliv Rev 2001;53:341–58.
[3] Langer R. Drug delivery: drugs on target. Science 2001;293:58–9.
[4] Alonso MJ. Nanomedicines for overcoming biological barriers. Biomed Pharmacother 2004;58:168–72.
[5] Pedersen N, Hansen S, Heydenreich AV, Kristensen HG, Poulsen HS. Solid lipid nanoparticles can effectively bind DNA, streptavidin and biotinylated ligands. Eur J Pharm Biopharm 2006;62:155–62.
[6] Wang Y, Gao SJ, Ye WH, Yoon HS, Yang YY. Co-delivery of drugs and DNA fromcationic core-shell nanoparticles self-assembled from a biodegradable copolymer. Nat Mater 2006;5:791–6.
[7] Zhang XH, Louise C, Sawyer GJ, Dong XB, Qiu Y, Fabre JW. In vivo gene delivery via portal vein and bile duct to individual lobes of the rat liver using a polylysine-based nonviral DNA vector in combination with chloroquine. Hum Gene Ther 2001;12:2179–90.
[8] Kishida T, Asada H, Itokawa Y, Yasutomi K, Shin-Ya M, Gojo S, et al. Electrochemo-gene therapy of cancer: intratumoral delivery of interleukin-12 gene and bleomycin synergistically induced therapeutic immunity and suppressed subcutaneous and metastatic melanomas in mice. Mol Ther 2003;8:738–45.
[9] Torrado S, Prada P, de la Torre PM, Torrado S. Chitosan-poly(acrylic) acid polylonic complex: in vivo study to demonstrate prolonged gastric retention. Biomaterials 2004;25:917–23.
[10] Yessine MA, Dufresne MH, Meier C, Petereit HU, Leroux JC. Proton-actuated membrane-destabilizing polyion complex micelles. Bioconjugate Chem 2007;18:1010–4.
[11] de la Torre PM, Enobakhare Y, Torrado G, Torrado S. Release of amoxicillin from polyionic complexes of chitosan and poly(acrylic acid): study of polymer/polymer and polymer/drug interactions within the network structure. Biomaterials 2003;24:1499–506.
[12] Chellat F, Tabrizian M, Dumitriu S, Chornet E, Magny P, Rivard CH, et al. In vitro and in vivo biocompatibility of chitosan–xanthan polyionic complex. J Biomed Mater Res 2000;51:107–16.
[13] Choi JS, Lee EJ, Choi YH, Jeong YJ, Park JS. Poly(ethylene glycol)-block-poly(L-lysine) dendrimer: novel linear polymer/dendrimer block copolymer forming a spherical water-soluble polyionic complex with DNA. Bioconjugate Chem 1999;10:62–5.
[14] Cohen H, Levy RJ, Gao J, Fishbein I, Kousaev V, Sosnowski S, et al. Sustained delivery and expression of DNA encapsulated in polymeric nanoparticles. Gene Ther 2000;7:1896–905.
[15] Panyam J, Zhou WZ, Prabha S, Sahoo SK, Labhasetwar V. Rapid endo-lysosomal escape of poly(DL-lactide-co-glycolide) nanoparticles: implications for drug and gene delivery. Faseb J 2002;16:1217–26.
[16] Gröhn F, Antonietti M. Intermolecular structure of spherical polyelectrolyte microgels in salt-free solution. 1. Quantification of the attraction between equally charged polyelectrolytes. Macromolecules 2000;33:5938–49.
[17] Oh JK, Tang C, Gao HF, Tsarevsky NV, Matyjaszewski K. Inverse miniemulsion ATRP: a new method for synthesis and functionalization of well-defined water-soluble/cross-linked polymeric particles. J Am Chem Soc 2006;128:5578–84.
[18] Akiyoshi K, Deguchi S, Tajima H, Nishikawa T, Sunamoto J. Microscopic structure and thermoresponsiveness of a hydrogel nanoparticle by self-assembly of a hydrophobized polysaccharide. Macromolecules 1997;30:857–61.
[19] Oh JK, Siegwart DJ, Lee H, Sherwood G, Peteanu L, Hollinger JO, et al. Biodegradable polyionic complexes prepared by atom transfer radical polymerization as potential drug delivery carriers: synthesis, biodegradation, in vitro release, and bioconjugation. J Am Chem Soc 2007;129:5939–45.
[20] Yu S, Hu JH, Pan XY, Yao P, Jiang M. Stable and pH-sensitive nanogels prepared by self-assembly of chitosan and ovalbumin. Langmuir 2006;22:2754–9.
[21] Li J, Yu SY, Yao P, Jiang M. Lysozyme–Dextran core-shell nanogels prepared via a green process. Langmuir 2008;24:3486–92.

[22] Yu SY, Yao P, Jiang M, Zhang GZ. Nanogels prepared by self-assembly of oppositely charged globular proteins. Biopolymers 2006;83:148–58.
[23] Hu JH, Yu SY, Yao P. Stable amphoteric nanogels made of ovalbumin and ovotransferrin via self-assembly. Langmuir 2007;23:6358–64.
[24] Sanda F, Terada K, Masuda T. Synthesis, chiroptical properties, and pH responsibility of aspartic acid- and glutamic acid-based helical polyacetylenes. Macromolecules 2005;38:8149–54.
[25] Bozkir A, Saka OM. Chitosan-DNA nanoparticles: effect on DNA integrity, bacterial transformation and transfection efficiency. J Drug Target 2004;12:281–8.
[26] Panyam J, Labhasetwar V. Biodegradable nanoparticles for drug and gene delivery to cells and tissue. Adv Drug Deliv Rev 2003;55:329–47.
[27] Govender T, Stolnik S, Garnett MC, Illum L, Davis SS. PLGA nanoparticles prepared by nanoprecipitation: drug loading and release studies of a water soluble drug. J Controlled Release 1999;57:177–85.
[28] Avgoustakis K. Pegylated poly(lactide) and poly(lactide-co-glycolide) nanoparticles: preparation, properties and possible applications in drug delivery. Curr Drug Deliv 2004;1:321–33.
[29] Mansouri S, Cuie Y, Winnik F, Shi Q, Lavigne P, Benderdour M, et al. Characterization of folate-chitosan-DNA nanoparticles for gene therapy. Biomaterials 2006;27:2060–5.
[30] Conwell CC, Huang L. Recent advances in non-viral gene delivery. Adv Genet 2005;53:1–18.